

PROJECT REPORT

On

**“SYNTHESIS AND CHARACTERIZATION OF SILVER
NANOPARTICLES INCORPORATED NANOHYDROXYAPATITE
FROM BIOMATERIALS AND ITS APPLICATION”**

Submitted by
ANUSREE AJAY
AM20CHE003

*In partial fulfillment for the award of the
Post graduate Degree in Chemistry*



**DEPARTMENT OF CHEMISTRY
AND
CENTRE FOR RESEARCH**

**ST. TERESA'S COLLEGE (AUTONOMOUS)
ERNAKULAM
2020-2022**

**DEPARTMENT OF CHEMISTRY
AND
CENTRE FOR RESEARCH
ST. TERESA'S COLLEGE (AUTONOMOUS)
ERNAKULAM**



M.Sc. CHEMISTRY PROJECT REPORT

Name : ANUSREE AJAY

Register Number : AM20CHE003

Year of Work : 2020-2022

This is to certify that the project “**SYNTHESIS AND CHARACTERIZATION OF SILVER NANOPARTICLES INCORPORATED NANOHYDROXYAPATITE FROM BIOMATERIALS AND ITS APPLICATION**” is the work done by **ANUSREE AJAY**.

Dr. JAYA T VARKEY
Head of the Department

Dr. JAYA T VARKEY
Staff-member in charge

Submitted to the Examination of Master's degree in Chemistry

Date:

Examiners:

:

**DEPARTMENT OF CHEMISTRY
AND
CENTRE FOR RESEARCH**

**ST. TERESA'S COLLEGE (AUTONOMOUS)
ERNAKULAM**



CERTIFICATE

This is to certify that the project work entitled “**SYNTHESIS AND CHARACTERIZATION OF SILVER NANOPARTICLES INCORPORATED NANOHYDROXYAPATITE FROM BIOMATERIALS AND ITS APPLICATION**” is the work done by **ANUSREE AJAY** under the guidance of **Dr. JAYA T VARKEY, ASSOCIATE PROFESSOR, HOD**, Department of Chemistry and Centre for Research, St. Teresa's College, Ernakulam in partial fulfilment of the award of the Degree of Master of Science in Chemistry at St. Teresa's College, Ernakulam affiliated to Mahatma Gandhi University, Kottayam.

Dr. Jaya T Varkey
Project Guide

Dr. Jaya T Varkey
Head of the Department

**DEPARTMENT OF CHEMISTRY
AND
CENTRE FOR RESEARCH**

**ST. TERESA'S COLLEGE (AUTONOMOUS)
ERNAKULAM**



CERTIFICATE

This is to certify that the project work entitled **“SYNTHESIS AND CHARACTERIZATION OF SILVER NANOPARTICLES INCORPORATED NANOHYDROXYAPATITE FROM BIOMATERIALS AND ITS APPLICATION”** is the work done by **ANUSREE AJAY** under my guidance in the partial fulfilment of the award of the Degree of Bachelor of Science in Chemistry at St. Teresa's College (Autonomous), Ernakulam affiliated to Mahatma Gandhi University, Kottayam.

Dr. JAYA T VARKEY
Project Guide

DECLARATION

I hereby declare that the project work entitled “**SYNTHESIS AND CHARACTERIZATION OF SILVER NANOPARTICLES INCORPORATED NANOHYDROXYAPATITE FROM BIOMATERIALS AND ITS APPLICATION**” submitted to Department of Chemistry and Centre for Research, St. Teresa’s College (Autonomous) affiliated to Mahatma Gandhi University, Kottayam, Kerala is a record of an original work done by me under the guidance of **Dr.JAYA T VARKEY,ASSOCIATE PROFESSOR, HOD**, Department of Chemistry and Centre for Research, St. Teresa’s College (Autonomous), Ernakulam (Internal Guide). This project work is submitted in the partial fulfillment of the requirements for the award of the Degree of Master of Science in Chemistry.

ANUSREE AJAY

Acknowledgement

The success and final outcome of this project required a lot of guidance and assistance from many people and we are extremely fortunate to have got this all along the completion of our project work.

First of all we thank the God Almighty for being with us throughout all the days and helping us to complete the project successfully.

We respect and thank our project guide Dr.Jaya.T.Varkey, Associate Professor, Head of the Department , Department of Chemistry, St. Teresa's College (Autonomous) Ernakulum for directing us to a world of research and opportunities , we thank her for her guidance and constant supervision as well as for providing information regarding the project and also for her support in completing project.

We extend our sincere gratitude to Dr. Sr. Vineetha, Director and Dr.Lizzy Mathew Principal, St. Teresa's College (Autonomous), Ernakulum for their extend support and co-operation during our project work. We would like to thank all the teachers and non- teaching staffs of the Department of Chemistry, St. Teresa's College, Ernakulum for their support and cooperation during our entire project.

We also feel proud to have a group of good friends who offered us much needed help in completing this project.

ANUSREE AJAY

Contents

Chapter 1: Introduction	1
1.1. Nanochemistry	2
1.2 Applications of Nanochemistry	3
1.2.1. Medicine	3
1.2.2. Catalysis	3
1.2.3. Wounds	3
1.3 Nanohydroxyapatite	4
1.4 Green synthesis of Nanoparticles	6
1.4.1 Green synthesis of silver nanoparticles	7
1.5 Application of silver nanoparticles	8
1.6 Silver incorporated Nano hydroxyapatite	11
Chapter 2: Materials and Methods	14
2.1 Characterization techniques	14
2.1.1 X-Ray Diffraction analysis	15
2.1.2 FTIR- Spectroscopy	17
2.1.3 Scanning Electron Microscopy	18
2.2 Synthesis of Nano hydroxyapatite from egg shells	20

2.3 Synthesis of silver nanoparticles	21
2.3.1 Preparation of Plant extract	22
2.3.2 Preparation of silver nanoparticles	23
2.4 Synthesis of silver hydroxyapatite Nanocomposite	23
2.5 Antimicrobial studies	24
Chapter 3: Results and discussions	26
3.1 X-Ray diffraction studies of silver nanoparticles	26
3.2 X-Ray diffraction studies of Nano hydroxyapatite	29
3.3 X-Ray diffraction studies of silver incorporated nano hydroxyapatite	33
3.4 FTIR- Analysis	37
3.5 SEM Analysis	41
3.6 Antimicrobial Studies	43
Chapter 4: Conclusions	45
Reference	46

ABBREVIATION

1. Np - Nanoparticles
2. AgNP- Silver nanoparticles
3. nHA - Nanohydroxyapatite
4. nHA-AgNP - Silver incorporated nano hydroxyapatite
5. XRD – X-Ray Diffraction
6. FTIR – Fourier Transform Infrared Spectroscopy
7. SEM- Scanning Electron Microscopy

Chapter 1

Introduction

Abstract: The field of nanotechnology is the most active area of research in modern materials science. Though there are many chemical as well as physical methods, green synthesis of nanomaterials is the most emerging method of synthesis. The Plant-mediated synthesis of nanoparticles is a green chemical approach that connects nanotechnology with plants. Novel methods of ideally synthesizing NPs are thus thought that are formed at ambient temperatures, neutral pH, low costs and environmentally friendly fashion. Keeping these goals in view nanomaterials have been synthesized using various routes.

The aim of the present study is to prepare, characterize and evaluate of silver nanoparticles incorporated nanohydroxyapatite as implants for bone defects and deformation. Hydroxyapatite is a naturally occurring rare mineral, but its most common occurrence is as the main inorganic constituent of natural bone and teeth mineral. It has excellent biocompatibility, bioactivity. Nanohydroxyapatite was isolated from egg shells and silver nanoparticles were prepared from Tulasi. The silver nanoparticles were incorporated into the prepared nanohydroxyapatite and the synthesis was confirmed by the characterization such as XRD, FTIR, SEM. The present study also focuses on the application of the synthesized nHA-AgNP composite for its antibacterial activity.

1.1 NANOCHEMISTRY

Nanochemistry is the combination of Chemistry and Nano science. It is associated with synthesis of building blocks which are dependent on size, surface, shape and defect properties. It is being used in chemical, materials and physical, science as well as engineering, biological and medical applications. This also involves the study of synthesis and characterisation of materials of Nano scale size. It is relatively a new branch of chemistry that is concerned with unique properties associated with assemblies of atoms or molecules of nano scale size (1-100nm)so the nanoparticles lie somewhere between individual atoms or molecules of bulk materials[1].It has uses in chemical, physical and materials science, engineering and biological and medical applications. Using single atoms as building blocks offers new ways to create innovative materials, the opportunity to create the smallest features possible in integrated circuits and the chance to explore quantum computing for example. It might seem relatively new, but nanochemistry has been employed for many years, for example in sunscreens that absorb UV light, in clear coatings for cars which protect the bright paint colours underneath, or in carbon nanotubes for lightweight car parts or sporting equipment. It has been used to study the health and safety effects of airborne and waterborne nanosized particulates, and nanoparticles have been used to clear up or neutralizes pollutants.

1.2 APPLICATIONS OF NANOCHEMISTRY

1.2.1 Medicine

One highly explained application of nanochemistry in medicine. A simple skin-care product using the technology of nanochemistry is sunscreen. Sunscreen contains nanoparticles of zinc oxide and titanium dioxide. These chemicals protect the skin against harmful UV light by absorbing or reflecting the light and prevent the skin from retaining full damage by photoexcitation of electrons in the nanoparticle. Effectively, the excitation of the particle blocks skin cells from DNA damage [2].

1.2.2 Catalysis

Nanoenzymes

Nanostructure materials mainly used in nanoparticle-based enzymes have drawn attraction due to the specific properties they show. Very small size of these nanoenzymes (or nanozymes) (1–100 nm) have provided them unique optical, magnetic, electronic, and catalytic properties. Moreover, the control of surface functionality of nano particles and predictable nanostructure of these small sized enzymes have made them to create a complex structure on their surface which in turn meet the needs of specific applications[3].

1.2.3 Wounds

For abrasions and wounds, Nano chemistry has demonstrated applications in improving the healing process. Electro spinning is a polymerization method used biologically in tissue engineering, but can be functionalized for wound dressing as well as drug delivery. This produces Nano fibers which encourage cell proliferation, antibacterial properties, and controlled

environment. These properties have been created in macroscale; however, nanoscale versions may show improved efficiency due to nanotopographical features[4]. Targeted interfaces between nanofibers and wounds have higher surface area interactions and are advantageously in vivo [5]. There is evidence certain nanoparticles of silver are useful to inhibit some viruses and bacteria. New developments in nanochemistry provide a variety of nanostructure materials with significant properties that are highly controllable. Some of the application of these nanostructure materials include self-assembled monolayers and lithography, use of nanowires in sensors, and nanoenzyme.

1.3 NANOHYDROXYAPATITE

Hydroxyapatite is one of the most studied biomaterials in the medical field for its proven biocompatibility and for being the main constituent of the mineral part of bone and teeth. In terms of restorative and preventive dentistry, nanohydroxyapatite has significant re-mineralizing effects on initial enamel lesions, certainly superior to conventional fluoride, and good results on the sensitivity of the teeth. The nano-HA has also been used as an additive material, in order to improve already existing and widely used dental materials, in the restorative field (experimental addition to conventional glass ionomercements, that has led to significant improvements in their mechanical properties). Because of its unique properties, such as the ability to chemically bond to bone, to not induce toxicity or inflammation and to stimulate bone growth through a direct action on osteoblasts, nano-

HA has been widely used in periodontology and in oral and maxillofacial surgery. Its use in oral implantology, however, is a widely used practice established for years, as this substance has excellent osteoinductive capacity and improves bone-to-implant integration. Calcium orthophosphate based inorganic materials are used widely in medicine and bone tissue engineering [6]. Among them, synthetic hydroxyapatite is the most promising due to its composition and chemical structure. This has the structure similar to the mineral phase of bone [6,7]. This ceramic has been used for repairing and reconstructing bone fractures as well as for coating orthopaedic, maxillofacial and dental implants. However, one of the biggest current problems in the biomedical field is post-surgical infections arising from recent-implanted synthetic biomaterials, since these provide sites for potential bacterial adhesion. Such infections often lead to severe pain and also it causes bone tissue loss in the body. To overcome the limitations of antibiotics used in prevention and treatment of these infections that might lead to highly resistant bacteria. Special attention is dedicated in controlling the release of alternative antimicrobial agents, such as copper, zinc and silver, which having wide activity and low bacterial resistance [8]. Several studies involving chemical synthesis reported the effect of chemical elements into biomaterials in order to obtain antimicrobial effects. Silver has been the most common due to its strong and non selective antibacterial activity [8]-[10]. Furthermore, the reactivity of silver is even more efficient when used in nano meter-sized particles due to their high surface-to volume ratio that allows better contact with microorganisms.

1.4 GREEN SYNTHESIS OF NANOPARTICLES

Green chemistry (sustainable chemistry): Design of chemical products and processes that reduce or eliminate the use or generation of substances hazardous to humans, animals, plants, and the environment. Green chemistry discusses the engineering concept of pollution prevention and zero waste both at laboratory and industrial scales. It encourages the use of economical and ecocompatible techniques that not only improve the yield but also bring down the cost of disposal of wastes at the end of a chemical process.

In materials science, “green” synthesis has gained extensive attention as a reliable, sustainable, and eco-friendly protocol for synthesizing a wide range of materials/nanomaterials including metal/metal oxides nanomaterials, hybrid materials. As such, green synthesis is regarded as an important tool to reduce the destructive effects associated with the traditional methods of synthesis for nanoparticles commonly utilized in laboratory and industry. Green synthesis’ are required to avoid the production of unwanted or harmful by-products through the build-up of reliable, sustainable, and eco-friendly synthesis procedures. The use of ideal solvent systems and natural resources (such as organic systems) is essential to achieve this goal. Green synthesis of metallic nanoparticles has been adopted to accommodate various biological materials (e.g., bacteria, fungi, algae, and plant extracts). Among the available green methods of synthesis for metal/metal oxide nanoparticles, utilization of plant extracts is a rather simple and easy process to produce nanoparticles at large scale. Green synthesis of nanoparticles has many potential applications in environmental and biomedical fields. The plants are considered to be more suitable compared to microbes for green synthesis of nanoparticles as they are non-pathogenic and various pathways are

thoroughly researched . A wide spectrum of metal nanoparticles has been produced using different. These nanoparticles have unique optical, thermal, magnetic, physical, chemical, and electrical properties [11]

1.4.1 GREEN SYNTHESIS OF SILVER NANOPARTICLES

Plant extract mediated synthesis always takes place extracellularly, and the reaction times have also been reported to be very short compared to that of microbial synthesis. Most importantly, the process can be suitably scaled up for large scale synthesis of NPs

Many plants such as *Pelargonium graveolens* [13], *Medicagosativa* [14], *Azadirachtaindica* [12], *Lemongrass* [15], *Aloe vera* [16], *CinnamomumCamphora* , *Emblicaofficinalis* , *Capsicum annum* , *Diospyros kaki* , *Carica papaya* [17], *Coriandrum* sp. [18], *Boswelliaovalifoliolata* [19], *Tridaxprocumbens*, *Jatrophacurcas*, *Solanummelongena*, *Daturametel*, *Citrus aurantium* [20], and many weeds have shown the potential of reducing silver nitrate to give formation of AgNPs.

Ocimum sanctum (Tulsi) is a medicinal herb abundantly found and cultured in India, Malaysia, Australia, West Africa, and some of the Arab countries [21]. Tulsi leaves have been traditionally used for treatment of many infections. The antibacterial activity has been reported to be the upshot of essential oil components, mostly eugenols found in it. The present study aims at the synthesis of silver nanoparticles from the aqueous extract of Tulsileaves. We also attempt to combine the inherent antimicrobial activities of silver metal and Tulsi extract for enhanced antimicrobial activity.

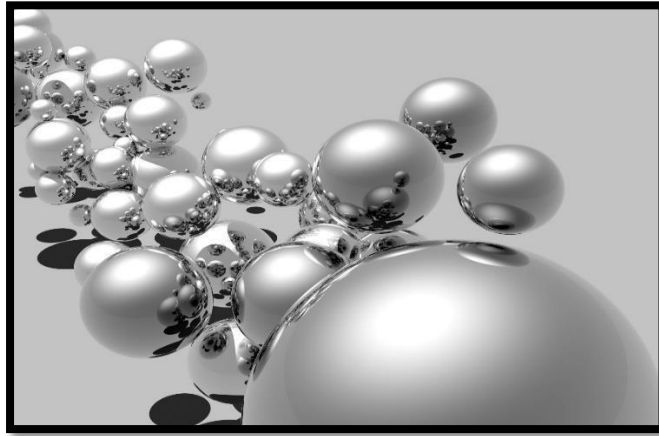


Figure 1: Silver nanoparticles

1.5 APPLICATIONS OF SILVER NANOPARTICLES

1.5.1 Nanoparticles are useful tools for various dental applications. They are used in dentistry for production of various biomaterials used in different dental application due to its antimicrobial properties

Oral cavity is a gateway to the entire the body and protection of this gateway is a major goal in dentistry. Plaque biofilm is a major cause of majority of dental diseases and although various biomaterials Nanoparticle applications have become useful tools have been applied for their cure for various dental applications in endodontics, periodontics, restorative dentistry, orthodontics and oral cancers. Off these, silver nanoparticles have been used in medicine and dentistry due to its antimicrobial properties. AgNps have been

incorporated into biomaterials in order to prevent or reduce biofilm formation due to greater surface to volume ratio and small particle size, they possess excellent antimicrobial action without affecting the mechanical properties of the material. This unique property of AgNps makes these materials as fillers of choice in different biomaterials whereby they play a vital role in improving the properties[22]

1.5.2. Silver nanoparticles are used in cotton fabric as an antibacterial impregnation method to provide the cotton fabric with antibacterial property.

A novel nano-silver colloidal solution was prepared in one step by mixing AgNO₃ aqueous solution and an amino-terminated hyperbranched polymer (HBP-NH₂) aqueous solution under vigorous stirring at room temperature. Cotton fabric was treated with nano-silver colloid by an impregnation method to provide the cotton fabric with antibacterial properties. The whiteness, silver content, antibacterial activity and washing durability of the silver-treated fabrics were determined. The results indicated that the silver-treated cotton fabric showed 99.01 % bacterial reduction of *Staphylococcus aureus* and 99.26 % bacterial reduction of *Escherichia coli* while the silver content on cotton was about 88 mg/kg. The antimicrobial activity of the silver-treated cotton fabric was maintained at over 98.77 % reduction level even after being exposed to 20 consecutive home laundering conditions. In addition, the results of scanning electron microscopy (SEM) and X-ray photoelectron spectroscopy (XPS) confirmed that silver nanoparticles have been fixed and well dispersed on cotton fabrics' surface and the major state of the silver presented on the surface was Ag⁰[23]

1.5.3 Silver nanoparticles are used in viral inhibition, a new hope for antivirals

Silver nanoparticles showed efficient antimicrobial property as compared to other salts due to their extremely large surface area. This enabled them to achieve better contact with the microorganisms. Nanoparticles get adsorbed onto the cell membrane and also penetrate inside the bacteria. Silver nanoparticles interact with sulphur containing proteins present in the cell membrane as well as the phosphorus containing compounds like DNA. When entry of silver nanoparticles takes place inside a bacterial cell it forms a low molecular weight region in the centre of the bacteria due to which the conglomerate. Thus shielding of the DNA with the silver ions and inhibiting replication the nanoparticles attacks the respiratory chain and bring the cell division to an end resulting in the cell death. The bacterial activity of silver ions gets enhanced when they are released from nanoparticles in the bacterial cell [24].

1.5.4. Applications of silver nanoparticles in food package.

Silver nanoparticles are antimicrobial agents that have a wide spectrum of action, against pathogenic bacteria and spoilage fungi. However, their mechanism of action is not completely clarified. Nowadays, scientific interest on biological synthesis of AgNPs is growing. AgNPs may be incorporated to biodegradable and non-biodegradable polymers for the production of food packages with antimicrobial properties, leading to greater safety and longer shelf life. However, it is important to carry out migration

tests for new food packages incorporated with AgNPs, based on the effective levels for their inclusion in the packaging materials [25].

1.6 SILVER INCORPORATED NANOHYDROXYAPATITE

A good approach to the treatment of implant-associated infections are the use of HA coatings for antibiotics delivery, this exploiting the osteoconductive properties of this material. However, the loading and release rate of antibiotics is strongly dependent on the acidic or basic character of antibiotics. Acidic antibiotics have greater efficiency than basic antibiotics because of the calcium-chelating properties of the carboxylate groups. However, through this calcium-carboxylate chelating interactions, the acidic antibiotics are retained to a greater extent than the basic antibiotics [26]. This fact imposes certain limitations in cases that require the use of acidic antibiotics, for example amoxicillin. Certain bacterial strains has a capacity to develop resistance against antibiotics. This capacity leads to an increasing interest for the controlled delivery of other antibacterial agents with a broader activity and low incidence of resistance. The metals such as silver or zinc, being an alternative strategy to avoid the formation of adhesive bacterial films [27]. The antibacterial properties of silver at low concentrations over a wide range of pathogens, including the common bacterial strains involved in implant-associated infections as well as the lack of toxicity for the mammalian cells, are well known [28–33]. Most silver-containing antimicrobial biomaterials consist of either elemental silver or Ag⁺ (silver salts or silver complexes) incorporated into organic (polymers) or inorganic (bioglasses and HA) matrices. While the in vitro antimicrobial

activity of silver-containing polymers (polyamides, polyurethane, and PMMA) and bioglasses has been extensively studied [34–37], but the bactericide action of Ag-HA materials has been reported in less extension. Recent reports says that, Ag-loaded HA composites obtained by ion-exchange methods (sol-gel or coprecipitation) [38–41].

These routes involve the silver substitution for calcium, resulting in a Ca-deficient hydroxyapatite. The antimicrobial response of these materials is good, but they have two main drawbacks:

- (i) The depletion of calcium could have negative effects on the structural stability of nano HA [40] as well as on its osteoconduction ability [41];
- (ii) A rapid release of silver, depending on the pH, can take place.

These facts have brought out an increasing interest on silver nanoparticles as bactericidal reservoir due to their low solubility in aqueous media. Studies on nanosilver-loaded polymer films reveal that the duration of silver release is strongly dependent on the total amount of silver nanoparticles [28]. The biocide activity of colloidal silver nanoparticles is influenced by their size—the smaller the particles, the greater antimicrobial effect [31]—however, the aggregation problems of nanoparticles are well known. A common solution to avoid this disadvantage is to support the nanoparticles on the surface of different substrates. Despite the potential clinical applications of nHA-Ag composites due to the combination of osteoconductive and bactericide properties, there are few examples in the literature of silver nanoparticles supported onto hydroxyapatite particles. These materials have been obtained by cosputtering of silver and hydroxyapatite to form coatings on titanium

surfaces [42], and by in situ reduction of silver cations on the surface of HA particles [43]. In the present work, a simple and low-cost method to support silver on the surface of hydroxyapatite to obtain a nano hybrid composite, containing 1 wt% of elemental silver, with antimicrobial activity is presented.

Chapter 2

Materials and Methods

This chapter gives a brief description of the materials and experimental procedures adopted for the present investigation.

Materials Required

- Orthophosphoric acid
- Egg shells
- Tulasi
- Silver Nitrate

2.1 CHARACTERIZATION TECHNIQUES

Characterization, when used in material science, refers to the use of external techniques to probe into the internal structure and properties of a material. Characterization can take the form of actual materials testing or analysis. Analysis techniques are used to simplify to magnify the specimen, to visualise its internal structure, and to gain knowledge as to the distribution of elements within the specimen and their interactions.

2.1.1 X-RAY DIFFRACTION ANALYSIS

The Definition of x-ray diffraction is: Diffraction of light means the bending of light around the corner of an obstacle. It is a fact that for diffraction to occur. The size of the obstacle should nearly be equal to the wavelength of light used. X-ray, like other electromagnetic rays, can also be diffracted, but for the diffraction of X-ray. The size of the obstacle should be a few angstroms (approx 1 \AA) which is approximately the wavelength of X rays. Since the atomic spacing in the Crystal is nearly a few \AA .

X-ray diffraction is based on constructive interference of monochromatic X-rays and a crystalline sample. These X-rays are generated by a cathode ray tube, filtered to produce monochromatic radiation, collimated to concentrate, and directed toward the sample. When a monochromatic x-ray incident occurs on a crystal. The atomic electrons in the Crystal are sent into vibration. With the same frequency as that of the frequency of the incident ray and are accelerated. These Accelerated electrons then emit the radiation of the same frequency as that of incident x-rays in all directions. If the wavelength of incident radiation is large compared to the dimensions of the Crystal. Then the radiated X-ray are in phase with each. But since the atomic dimension are nearly equal to the wavelength of X-Ray. The radiation emitted by the electrons is out of phase with each other. These radiations may interfere constructively or destructively producing a diffraction pattern (i.e. maxima and minima) in certain directions

Bragg's Law of Diffraction

In order to explain the diffraction of x rays, W.L. Bragg considered the X-ray diffraction from a crystal as a problem of reflection of X-rays from the atomic planes of the crystal in accordance with the laws of reflection. Consider a set of parallel atomic planes of the Crystal with Miller Indices $[hkl]$, such that the distance between the two successive planes is d . Let a parallel beam of monochromatic X-rays of wavelength λ be incident on the Plane at a glancing angle θ such that the incident rays lie in the plane of the paper.

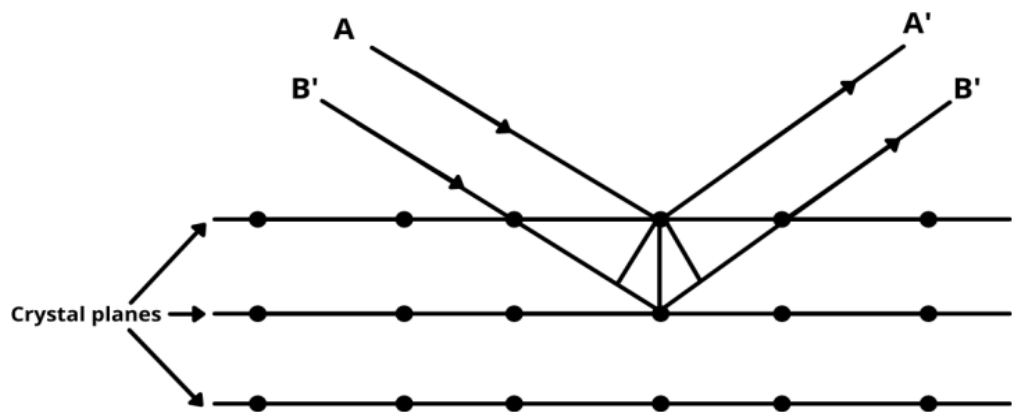


Figure 2: XRD

Let AP and BQ be two parallel incident rays that are reflected from points P and Q on the Crystal planes and travel along with PA' and QB' respectively.

If the path difference between APA' and BQB' is an integral multiple of λ , there will be constructive interference and a maximum will be observed [44].

2.1.2 FTIR SPECTROSCOPY

Fourier transform infrared spectrometer (FTIR) is one of the instruments based on infrared spectroscopy. It is the most modern type and preferred over the other dispersive spectrometers. It is because of its high precision, accuracy, speed, enhanced sensitivity, ease of operation, and sample non destructiveness. The fundamental of infrared spectroscopic technology is on atomic vibrations of a molecule that only absorbs specific frequencies and energies of infrared radiation. The molecules could be detected and classified by FTIR because different molecules will have different infrared spectrum. A block diagram of FTIR working process is shown in Figure 3. The FTIR spectrometer essentially uses an interferometer to measure the energy that is being transmitted to the sample. The infrared radiation emitted from the black body reaches the interferometer where the spectral encoding of signals happens. The resultant interferogram signal is transmitted through or bounces from the sample surface, where specific energy wavelengths are absorbed. The beam eventually passes through the detector and further passed on to processing computer for Fourier transformation of energy signals [45]

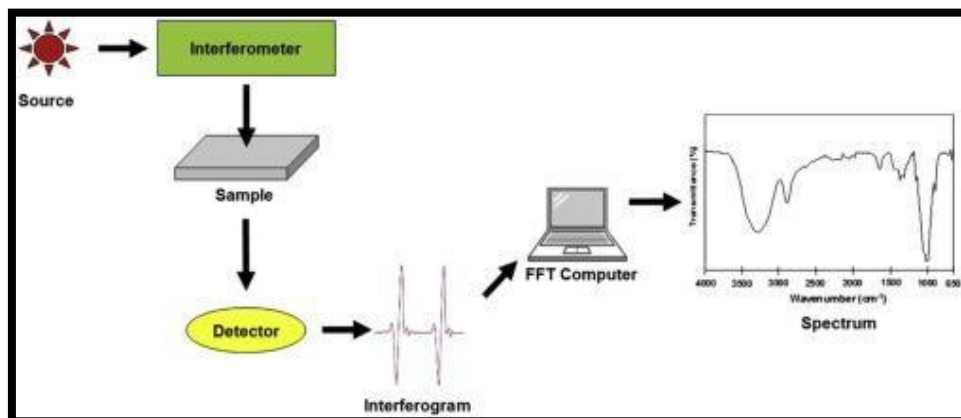


Figure3: FTIR block diagram

2.1.3 SCANNING ELECTRON MICROSCOPE

A scanning electron microscope (SEM) is a type of electron microscope that produces images of a sample by scanning the surface with a focused beam of electrons. The electrons interact with atoms in the sample, producing various signals that contain information about the surface topography and composition of the sample. The electron beam is scanned in a raster scan pattern, and the position of the beam is combined with the intensity of the detected signal to produce an image. In the most common SEM mode, secondary electrons emitted by atoms excited by the electron beam are detected using a secondary electron detector (Everhart-Thornley detector). The number of secondary electrons that can be detected, and thus the signal intensity, depends, among other things, on specimen topography. Some SEMs can achieve resolutions better than 1 nanometre. Specimens are observed in high vacuum in a conventional SEM, or in low vacuum or wet conditions in a variable pressure or environmental SEM, and at a wide range

of cryogenic or elevated temperatures with specialized instruments[46].The signals used by an SEM to produce an image result from interactions of the electron beam with atoms at various depths within the sample.

Various types of signals are produced including secondary electrons (SE), reflected or back-scattered electrons (BSE), characteristic X-rays and light (cathodoluminescence) (CL), absorbed current (specimen current) and transmitted electrons. Secondary electron detectors are standard equipment in all SEMs, but it is rare for a single machine to have detectors for all other possible signals. Secondary electrons have very low energies on the order of 50 eV, which limits their mean free path in solid matter .Consequently, SEs can only escape from the top few nanometers of the surface of a sample. The signal from secondary electrons tends to be highly localized at the point of impact of the primary electron beam, making it possible to collect images of the sample surface with a resolution of below 1 nm. Back-scattered electrons (BSE) are beam electrons that are reflected from the sample by elastic scattering. Since they have much higher energy than SEs, they emerge from deeper locations within the specimen and, consequently, the resolution of BSE images is less than SE images. However, BSE are often used in analytical SEM, along with the spectra made from the characteristic X-rays, because the intensity of the BSE signal is strongly related to the atomic number (Z) of the specimen. BSE images can provide information about the distribution, but not the identity, of different elements in the sample. In samples predominantly composed of light elements, such as biological specimens, BSE imaging can image colloidal gold immuno-labels of 5 or 10 nm diameter, which would otherwise be difficult or impossible to detect in secondary electron images [47].

Characteristic X-rays are emitted when the electron beam removes an inner shell electron from the sample, causing a higher-energy electron to fill the shell and release energy. The energy or wavelength of these characteristic X-rays can be measured by Energy-dispersive X-ray spectroscopy or Wavelength-dispersive X-ray spectroscopy and used to identify and measure the abundance of elements in the sample and map their distribution. Due to the very narrow electron beam, SEM micrographs have a large depth of field yielding a characteristic three-dimensional appearance useful for understanding the surface structure of a sample[48]. This is exemplified by the micrograph of pollen shown above. A wide range of magnifications is possible, from about 10 times (about equivalent to that of a powerful hand-lens) to more than 500,000 times, about 250 times the magnification limit of the best light microscopes.

2.2 SYNTHESIS OF NANOHYDROXYAPATITE FROM EGG SHELLS

Procedure

In the present study nanohydroxyapatite is synthesized using wet precipitation technique. Eggshells were collected, washed with distilled water, dried, then crushed and calcinated at 900°C for 2 hours. The decomposition of eggshell (CaCO_3) to CaO takes place. The freshly prepared CaO was mixed with the stoichiometric amount of distilled water to prepare $\text{Ca}(\text{OH})_2$. The 0.5M $\text{Ca}(\text{OH})_2$ suspension was vigorously stirred at 70°C for 1 hour and the 0.3M H_3PO_4 solution was added at the end of the stirring time

drop wise with a slow stirring rate. The pH of the solution was kept in the range 10.5-11. After complete addition of the H_3PO_4 solution, the contents were stirred for 1 hour at $70^\circ C$. The precipitate was washed with distilled water and dried in hot air oven at $105^\circ C$ for 24hours. The formed powder was calcinated at $900^\circ C$ for 2hour.

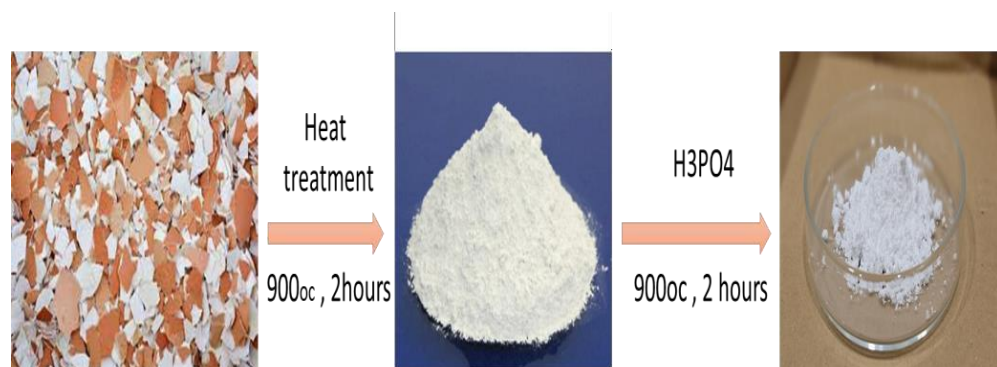


Figure 4 :Preparation of hydroxyapatite

2.3 SYNTHESIS OF SILVER NANOPARTICLES

In recent years silver nanoparticles have been investigated by many research groups nationally and internationally. It is mainly because of the potential application of nanoparticles in biology, medicine, optics and in modern electronic devices. Silver nanoparticles have advantage over other noble nanoparticles (e.g., gold and copper) Silver nanoparticles exhibit very strong bactericidal activity against gram-positive as well as gram negative bacteria including multi-resistant strains, as well as potential antifungal agent.

Material Required:

➤ Plant Sample: *Ocimumtenuiflorum* (Tulsi)

Kingdom : Plantae

Subkingdom :Tracheobionta

Superdivision :Spermatophyta

Division :Magnoliophyta

Class :Magnoliopsida

Subclass :Asteridae

Order :Lamiales

Family :Lamiaceae

Genus :Ocimum

Species : O. tenuifloram

Chemicals required: 1 Molar Silver nitrate (AgNO_3)

Procedure:**2.3.1. Preparation of plant extract**

Healthy plant samples were collected and cleaned properly in running tap water. The samples were allowed to dry at room temperature. About 40 grams of plant leaves were weighed out and were cut into small pieces. Finely cut pieces were then mixed with 200 ml distilled water. This mixture

was kept for boiling for 30 minutes. After cooling to room temperature, it was filtered using Whatman no- 40 filter paper.

2.3.2. Synthesis of Silver Nanoparticle

100 ml of aqueous solution of plant extract was added to 50 ml of 1 molar silver nitrate solution. The solution was allowed to react at room temperature. Silver nanoparticles formed were allowed to settle down. It is then filtered using Whatman no – 40 and then dried



Figure 5: Preparation of silver nanoparticles

2.4 Synthesis of silver hydroxyapatite Nanocomposite

To 25 ml of deionised water, 0.50 g nanohydroxyapatite powder was added and dissolved completely under vigorous magnetic stirring at 60°C. Then 0.25g silver nanoparticles were added to it stirred and allowed the reaction mixture to react overnight. The resulting sample was greenish brown in

colour. The sample was centrifuged at 5000 rpm to separate the silver incorporated hydroxyapatite nanocomposite precipitate.

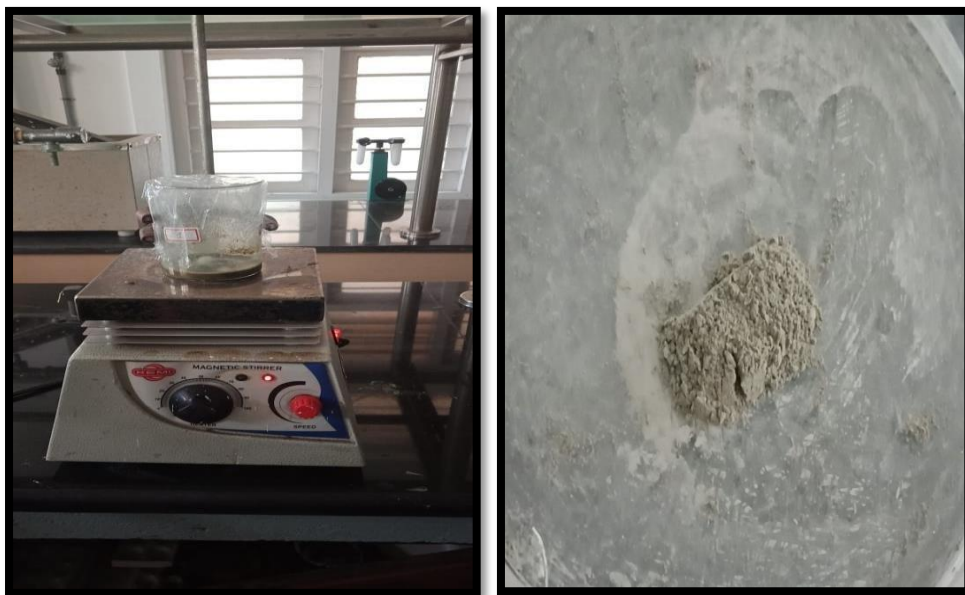


Figure 6 and 7: solution was stirred to obtain the silver incorporated nanohydroxyapatite

2.5 ANTIMICROBIAL STUDIES

ANTIMICROBIAL ASSAY BY DISC DIFFUSION METHOD

Procedure:

Using aseptic techniques, a single pure colony was transferred into a 10 ml of nutrient Broth and was placed in incubator at 37°C for overnight

incubation. Sterile MHA plates were prepared and the bacterial inoculum of *E.coli* and *Staphylococcus aureus* were uniformly swabbed in each plate. Test samples of volume 50µl added to the disc and were placed over the agar plates. The plates were incubated at 37°C for 18 hours a period sufficient for the growth. After incubation, the diameter of inhibitory zones formed around each well were measured in cm and recorded.

Chapter 3

RESULTS AND DISCUSSION

This chapter gives brief description of the experimental results obtained after doing the analysis - XRD, FTIR and SEM.

3.1 X-RAY DIFFRACTION STUDIES- SILVER NANOPARTICLES

The XRD pattern of the silver nanoparticles is shown in Fig 8

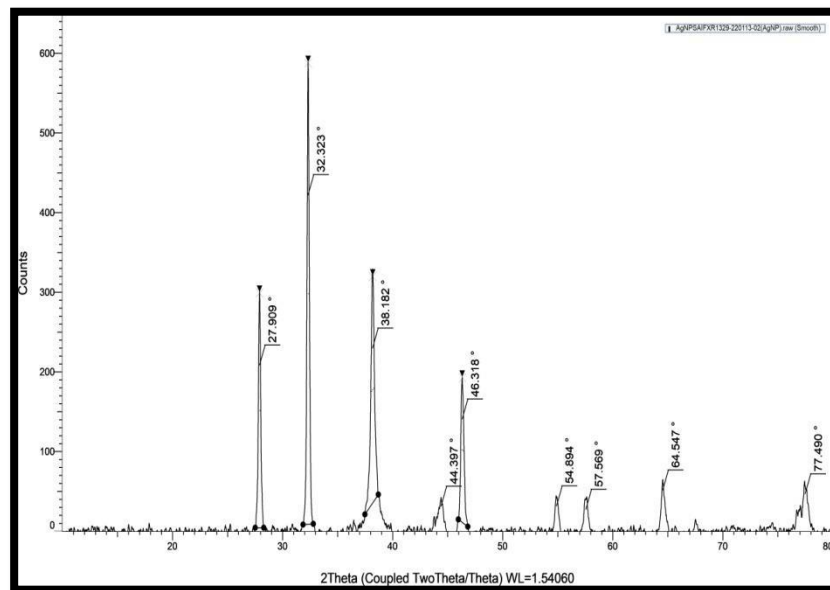


Figure 8: XRD pattern of AgNP

3.1.1 XRD- Particle Size Calculation

From this study, considering the peak at degrees, average particle size has been estimated by using Debye-Scherrer formula,

$$D = 0.9\lambda/B\cos\theta$$

where λ ' is the wave length of X-ray (0.1541nm), B' is FWHM (full width at half maximum), θ ' is the diffraction angle and D' is the particle diameter size and 'n' is the order of reflection. The calculated particle size details are in table.

Calculations- Particle size determination by XRD

1. Silver nanoparticles prepared from Tulasi

Peak-1:-

$$2\theta = 27.910^\circ$$

$$\theta = 13.955^\circ = 0.2434 \text{ radian}$$

$$B = 0.224 = 0.003909 \text{ radian}$$

$$\lambda = 1.5406 \times 10^{-10} \text{ m}$$

From Debye-scherrer equation,

$$D = 0.9\lambda/B\cos\theta = 0.9 \times 1.5406 \times 10^{-10} / 0.003909 \times \cos(0.2434) = 35.4707 \text{ nm}$$

Peak-2:-

$$2\theta = 32.329^\circ$$

$$\theta = 16.1645^\circ = 0.28198 \text{ radian}$$

$$B = 0.227 = 0.003962 \text{ radian}$$

$$\lambda = 1.5406 \times 10^{-10} \text{ m}$$

From Debye-scherrer equation,

$$D = 0.9\lambda/B\cos\theta = 0.9 \times 1.5406 \times 10^{-10} / 0.003962 \times \cos(0.28198) = 34.9963 \text{ nm}$$

Peak-3:-

$$2\theta = 38.188^\circ$$

$$\theta = 19.094^\circ = 0.3330 \text{ radian}$$

$$B = 0.345 = 0.006021 \text{ radian}$$

$$\lambda = 1.5406 \times 10^{-10} \text{ m}$$

From Debye-scherrer equation,

$$D = 0.9\lambda/B\cos\theta = 0.9 \times 1.5406 \times 10^{-10} / 0.006021 \times \cos(0.3330) = 23.0287 \text{ nm}$$

Peak-4:-

$$2\theta = 46.345^\circ$$

$$\theta = 23.1725^\circ = 0.4044 \text{ radian}$$

$$B = 0.314 = 0.00548 \text{ radian}$$

$$\lambda = 1.5406 \times 10^{-10} \text{ m}$$

From Debye-scherrer equation,

$$D = 0.9\lambda/B\cos\theta = 0.9 \times 1.5406 \times 10^{-10} / 0.00548 \times \cos(0.4044) = 25.3024 \text{ nm}$$

$$\text{Mean value} = (35.4707 + 34.9963 + 23.0287 + 25.3024) / 4 =$$

$$\mathbf{29.6995 \text{ nm}}$$

2 Θ of the intense peak	FWHM Of intense peak	Size of the particle (D) nm	Average particle size(nm)
27.910°	0.003909	35.4707	29.6995
32.329°	0.003962	34.9963	
38.188°	0.006021	23.0287	
46.345°	0.00548	25.3024	

Table 1: Average particle size of AgNP

The X-ray diffraction pattern of the silver nanoparticles is shown in Fig.8. The diffraction peaks are sharp which indicate that the crystalline nature is present. The size of the silver nanoparticles estimated from Debye– Scherrer formula (Instrumental broadening) is 29.6995nm.

3.2 X-RAY DIFFRACTION STUDIES- NANO HYDROXYAPATITE

The XRD pattern of the nanohydroxyapatite is shown in Fig: 9

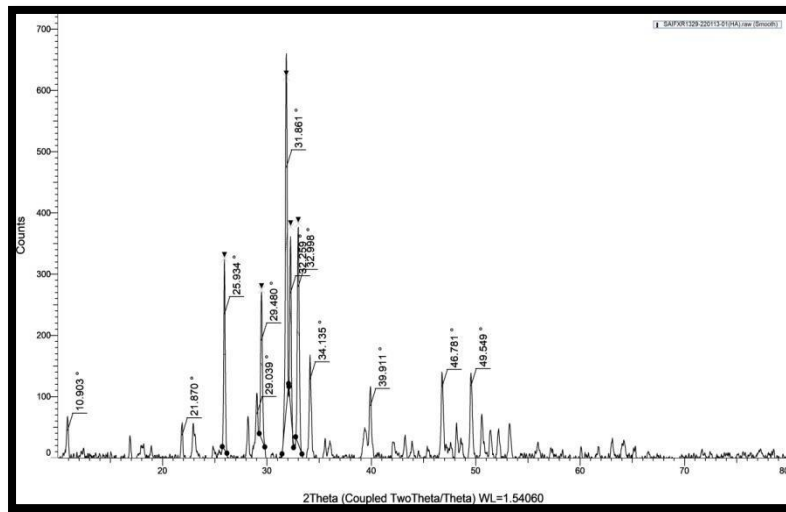


Figure 9: XRD pattern of Hydroxyapatite

3.2.1 XRD- Particle Size Calculation

From this study, considering the peak at degrees, average particle size has been estimated by using Debye-Scherrer formula,

$$D = 0.9\lambda/B\cos\theta$$

where λ' is the wave length of X-ray (0.1541nm), B' is FWHM (full width at half maximum), θ' is the diffraction angle and D' is the particle diameter size. The calculated particle size details are in table.

Hydroxyapatite prepared from Egg shells

Peak-1:-

$$2\theta = 25.936^\circ$$

$$\theta = 12.968^\circ = 0.2263 \text{ radian}$$

$$B = 0.153 = 0.00267 \text{ radian}$$

$$\lambda = 1.5406 \times 10^{-10} \text{ m}$$

From Debye-scherrer equation,

$$D = 0.9\lambda/B\cos\theta = 0.9 \times 1.5406 \times 10^{-10} / 0.00267 \times \cos(0.2263) = 51.9307 \text{ nm}$$

Peak-2:-

$$2\theta = 29.936^\circ$$

$$\theta = 14.968^\circ = 0.2612 \text{ radian}$$

$$B = 0.186 = 0.003246 \text{ radian}$$

$$\lambda = 1.5406 \times 10^{-10} \text{ m}$$

From Debye-scherrer equation,

$$D = 0.9\lambda/B\cos\theta = 0.9 \times 1.5406 \times 10^{-10} / 0.003246 \times \cos(0.2612) = 42.7157 \text{ nm}$$

Peak-3:-

$$2\theta = 31.862^\circ$$

$$\theta = 15.931^\circ = 0.2779 \text{ radian}$$

$$B = 0.198 = 0.003456 \text{ radian}$$

$$\lambda = 1.5406 \times 10^{-10} \text{ m}$$

From Debye-scherrer equation,

$$D = 0.9\lambda/B\cos\theta = 0.9 \times 1.5406 \times 10^{-10} / 0.003456 \times \cos(0.2779) = 40.1202 \text{ nm}$$

Peak-4:-

$$2\theta = 32.267^\circ$$

$$\theta = 16.1335^\circ = 0.2814 \text{ radian}$$

$$B = 0.153 = 0.00267 \text{ radian}$$

$$\lambda = 1.5406 \times 10^{-10} \text{ m}$$

From Debye-scherrer equation,

$$D = 0.9\lambda/B\cos\theta = 0.9 \times 1.5406 \times 10^{-10} / 0.00267 \times \cos(0.2814) = 51.9309 \text{ nm}$$

Peak-5:-

$$2\theta = 33.009^\circ$$

$$\theta = 16.5045^\circ = 0.2881 \text{ radian}$$

$$B = 0.199 = 0.003473 \text{ radian}$$

$$\lambda = 1.5406 \times 10^{-10} \text{ m}$$

From Debye-scherrer equation,

$$D = 0.9\lambda/B\cos\theta = 0.9 \times 1.5406 \times 10^{-10} / 0.003473 \times \cos(0.2881) = 39.9239 \text{ nm}$$

$$\text{Mean value} = (51.9307 + 42.7157 + 40.12020 + 51.9309 + 39.9239) / 5 =$$

$$\mathbf{45.32428 \text{ nm}}$$

2 Θ of the intense peak	FWHM Of intense peak	Size of the particle (D) nm	Average particle size(nm)
25.936°	0.00267	51.9307	45.32428
29.936°	0.003246	42.7157	
31.862°	0.003456	40.1202	
32.267°	0.00267	51.9309	
33.009°	0.003473	39.9239	

Table 2: Average particle size of AgNP

The X-ray diffraction pattern of the nanohydroxyapatite is shown in Fig.9. The diffraction peaks are sharp which indicate that the crystalline nature is present. The size of the nanohydroxyapatite estimated from Debye– Scherrer formula (Instrumental broadening) is 45.32428nm.

3.3 X-RAY DIFFRACTION STUDIES- SILVER INCORPORATED NANO HYDROXYAPATITE

The XRD pattern of the silver incorporated nanohydroxyapatite is shown in Fig: 10

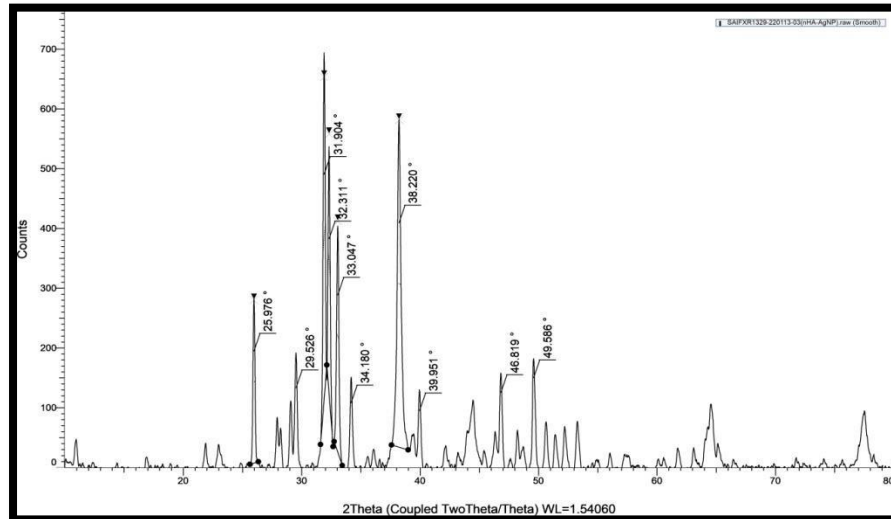


Figure 10: XRD pattern of AgNP-nHA

3.3.1 XRD- Particle Size Calculation

From this study, considering the peak at degrees, average particle size has been estimated by using Debye-Scherrer formula,

$$D = 0.9\lambda/B\cos\theta$$

where λ' is the wave length of X-ray (0.1541nm), B' is FWHM (full width at half maximum), θ' is the diffraction angle and D' is the particle diameter size. The calculated particle size details are in table.

Peak-1:-

$$2\theta = 25.974^\circ$$

$$\theta = 12.987^\circ = 0.2266 \text{ radian}$$

$$B = 0.189 = 0.003298 \text{ radian}$$

$$\lambda = 1.5406 \times 10^{-10} \text{m}$$

From Debye-scherrer equation,

$$D = 0.9\lambda/B\cos\theta = 0.9 \times 1.5406 \times 10^{-10} / 0.003298 \times \cos(0.2266) = 42.0422 \text{nm}$$

Peak-2:-

$$2\theta = 31.897^\circ$$

$$\theta = 15.9485^\circ = 0.2782 \text{radian}$$

$$B = 0.207 = 0.0036128 \text{radian}$$

$$\lambda = 1.5406 \times 10^{-10} \text{m}$$

From Debye-scherrer equation,

$$D = 0.9\lambda/B\cos\theta = 0.9 \times 1.5406 \times 10^{-10} / 0.0036128 \times \cos(0.2782) = 38.3789 \text{nm}$$

Peak-3:-

$$2\theta = 32.321^\circ$$

$$\theta = 16.1605^\circ = 0.2821 \text{radian}$$

$$B = 0.188 = 0.003281 \text{radian}$$

$$\lambda = 1.5406 \times 10^{-10} \text{m}$$

From Debye-scherrer equation,

$$D = 0.9\lambda/B\cos\theta = 0.9 \times 1.5406 \times 10^{-10} / 0.003281 \times \cos(0.2821) = 42.2602 \text{nm}$$

Peak-4:-

$$2\theta = 33.049^\circ$$

$$\theta = 16.5245^\circ = 0.2884 \text{ radian}$$

$$B = 0.211 = 0.003683 \text{ radian}$$

$$\lambda = 1.5406 \times 10^{-10} \text{ m}$$

From Debye-scherrer equation,

$$D = 0.9\lambda/B\cos\theta = 0.9 \times 1.5406 \times 10^{-10} / 0.003683 \times \cos(0.2884) = 37.6476 \text{ nm}$$

Peak-5:-

$$2\theta = 38.228^\circ$$

$$\theta = 19.114^\circ = 0.3336 \text{ radian}$$

$$B = 0.333 = 0.005812 \text{ radian}$$

$$\lambda = 1.5406 \times 10^{-10} \text{ m}$$

From Debye-scherrer equation,

$$D = 0.9\lambda/B\cos\theta = 0.9 \times 1.5406 \times 10^{-10} / 0.005812 \times \cos(0.3336) = 23.85691 \text{ nm}$$

$$\text{Mean value} = (42.0422 + 38.3789 + 42.2602 + 37.6476 + 23.85691) / 5 =$$

36.8372 nm

2 Θ of the intense peak	FWHM Of intense peak	Size of the particle (D) nm	Average particle size(nm)
25.974°	0.003298	42.0422	36.8372
31.897°	0.0036128	38.3789	
32.321°	0.003281	42.2602	
33.049°	0.003683	37.6476	
38.228°	0.005812	23.85691	

Table 3: Average particle size of AgNP

The X-ray diffraction pattern of the silver incorporated hydroxyapatite nano composite is shown in Fig.10. The diffraction peaks are sharp which indicate that the crystalline nature is present. The size of the silver nanoparticles estimated from Debye– Scherrer formula (Instrumental broadening) is 36.8372nm.

3.4 FTIR RESULT ANALYSIS

FT-IR analysis: FTIR spectroscopy was employed to characterize the different functional groups of the samples of AgNP, nHA and nHA-AgNP.

The spectrum was recorded in the range of 4500-500cm⁻¹.

3.4.1. FTIR SPECTRUM OF SYNTHESIZED AgNP

The absorption peak at 3431.52cm^{-1} is assigned to O-H stretch of alcohols and phenolic compounds of the leaf extract. The band at 2860.03cm^{-1} is attributed to C-H stretching of vibrations of methyl, methylene, and methoxy groups.

The absorption band at 1626.17cm^{-1} may be due to C=N bending in amide group or C=O stretching in carboxyl group.

The absorption band at 1626.17cm^{-1} is close to that reported for native proteins, which suggests that proteins acted as reducing and capping agents for the biosynthesis of AgNP.

The band at 1384.13cm^{-1} corresponds to C-O-C stretching mode of alcohols and carboxylic acids.

The peak at 1049.14cm^{-1} was assigned to the stretch of the C-O bond.

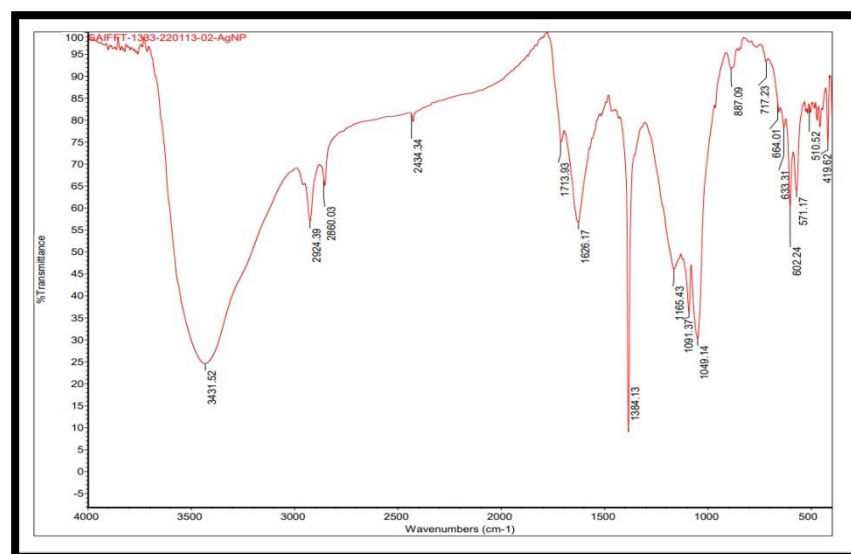


Figure 11: FTIR spectrum of AgNP

3.4.2. FTIR SPECTRUM OF nHA

The spectrum shows all characteristic absorption peak of nHA.

The first indication for the formation of nHA is in the form of a strong broad FTIR band centered at about 1046.20-1091.54 cm^{-1} due to asymmetric stretching mode of vibration for PO_4^{3-} .

The band about 569.00-602.80 cm^{-1} corresponds to symmetric P-O stretching vibration of the PO_4^{3-} . The crystalline powder generates two characteristic stretching modes of O-H bands at about 3571.72 cm^{-1} .

The broad band at 3437.18 cm^{-1} indicates adsorbed H₂O in the sample.

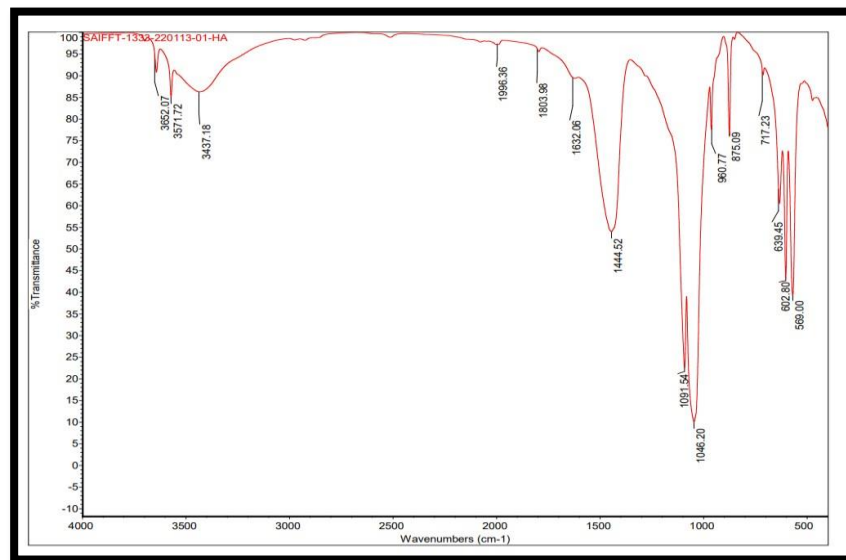


Figure12 : FTIR spectrum of nHA

3.4.3 FTIR SPECTRUM OF nHA-AgNP

The absorption band at 3574.30cm^{-1} in nHA, characteristic of OH stretching was shifted to 3427.62cm^{-1} in nHA –AgNP and infers greater interaction between the AgNP and nHA.

The absorption band at 1627.97cm^{-1} corresponds to the absorbed water and in evidence of the presence of absorbed water in the composite. The bands characteristics of PO_4^{3-} in nanohydroxyapatite structure are clearly observed at $632\text{-}475\text{cm}^{-1}$ and 711.09cm^{-1} . The small CO_2^- band was presented in spectra at 1452.29cm^{-1} .

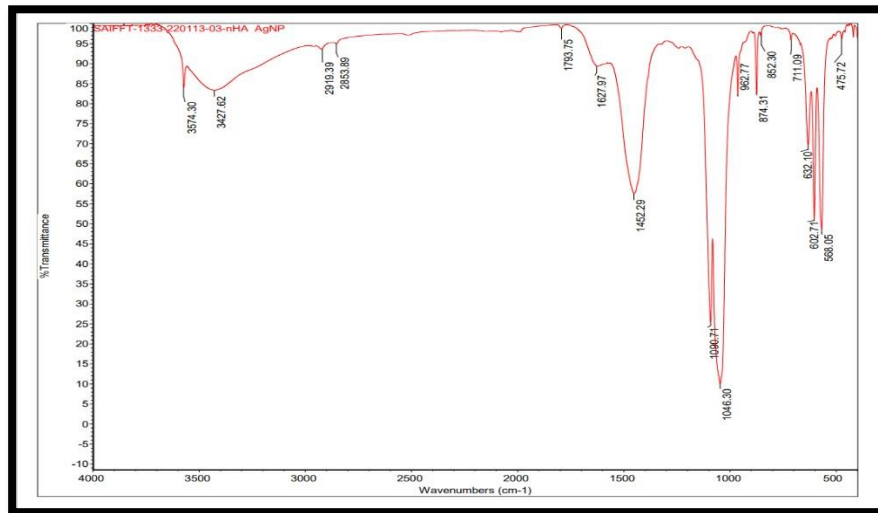


Figure 13: FTIR spectrum of AgNP-nHA

3.5 SEM Analysis

The surface morphology of AgNP, nHA and nHA-AgNP were analysed using SEM analysis. The SEM image of silver nanoparticles (Fig 14) shows that the nanoparticles are like crystal flakes in shape and the SEM image of nHA (Fig 15) shows that the particles are agglomerates of irregular shape, which have a tendency of leaving pores in between, the formation of pores are advantages since they permit tissue growth on implants inside the body when it is used as a biomaterial..

The SEM image of nHA-AgNP nanocomposite (Fig 16) shows that the particles of nHA-AgNP having both crystal flake shape with mild agglomeration confirming the biosynthesis of nHA-AgNP Nanocomposite.

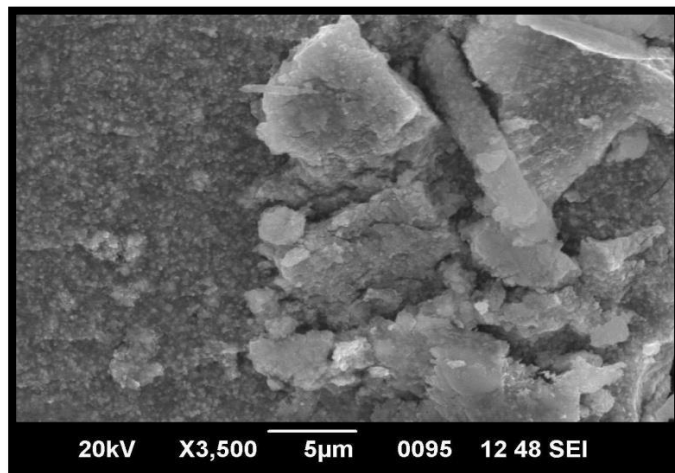


Figure 14: SEM image of AgNP

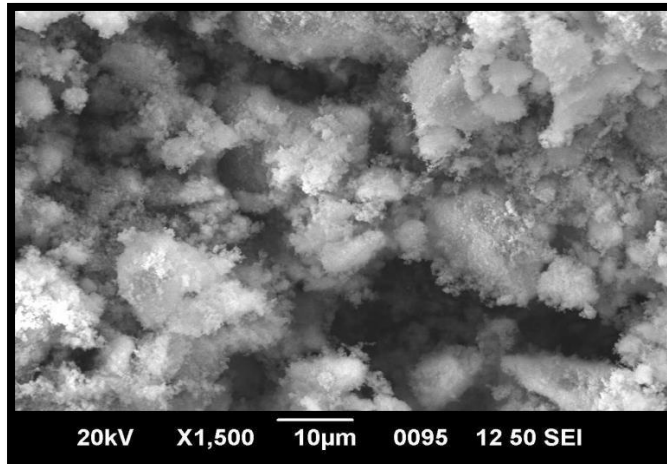


Figure 15: SEM image of nHA

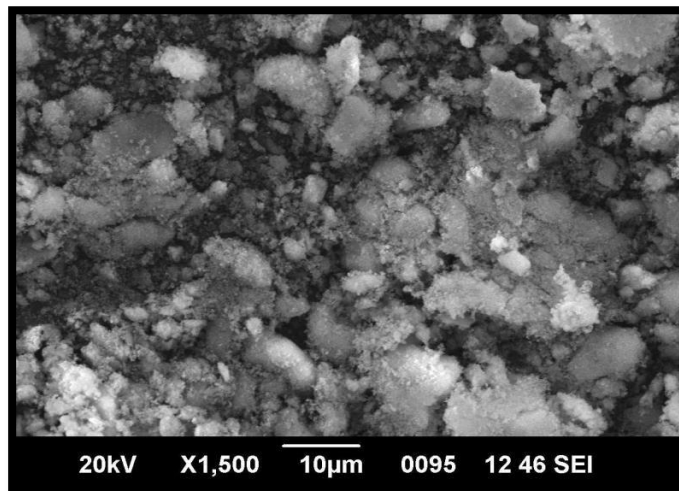


Figure 16: SEM image of nHA-AgNP nanocomposite

3.6 ANTIMICROBIAL STUDIES

The antibacterial studies was observed against staphylococcus aureus (gram-positive) and Escherichia coli (gram –negative).

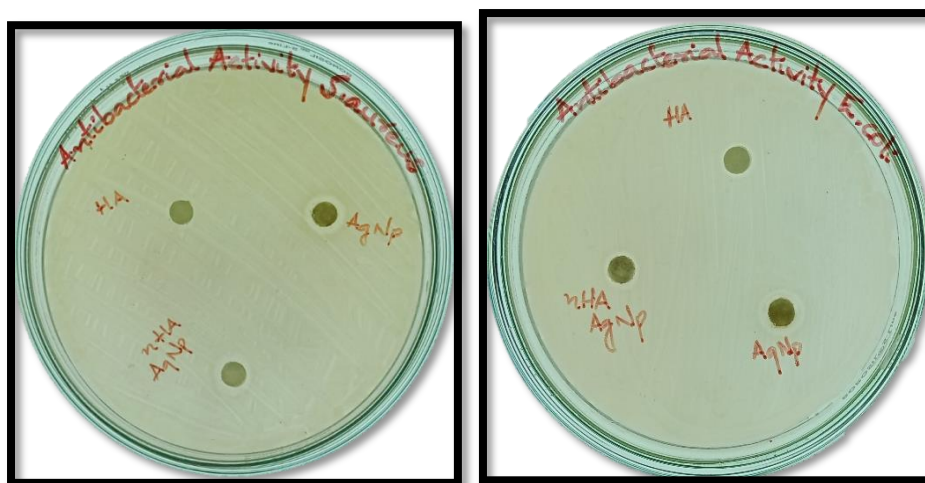


Figure 17: Antibacterial activity of synthesized AgNP ,nHA , nHA-AgNP against staphylococcus aureus and Escherichia coli

Disc Diameter = 0.5 cm

Organism	Sample	Zone of inhibition (cm)
<i>E.coli</i>	HA	No Zone
	nHA- AgNp	0.3 cm
	AgNp	0.5 cm
<i>Staphylococcus aureus</i>	HA	No Zone
	nHA-AgNp	0.2 cm
	AgNp	0.2 cm

Table4: Antimicrobial studies

All the three samples (AgNP ,nHA , nHA-AgNP) showed antibacterial activity against the two strains. In the case of Hydroxyapatite (nHA) did not show any zone of inhibition in both Ecoli and staphylococcus aureus. AgNP showed activity against staphylococcus aureus and Ecoli and it is clear that the incorporation of AgNP to nHA enhance the activity against both staphylococcus aureus and Ecoli. Thus the synthesized nHA-AgNP nanocomposite exhibited enhanced antibacterial activity and could be utilized for orthopedic and dental implants.

Chapter 4

CONCLUSION

The current work highlights the synthesis of silver incorporated with hydroxyapatite (nHA-AgNP) using wet precipitation method with versatile applications. This method is relatively convenient and cost effective to produce composite nHA-AgNP. In the present study nanohydroxyapatite was prepared from egg shells and the green synthesis of silver nanoparticles were prepared from Tulasi leaf extract. The green synthesis was confirmed using XRD, FTIR and SEM studies. The XRD result showed that AgNP, nHA, AgNP-nHA were successfully synthesized and the average particle size was found to be 29.6995nm, 45.32428nm, 36.8372nm which was calculated using Debye-Scherrer formula. The FTIR analysis indicate the presence of different functional groups in the prepared samples. The SEM images showed that AgNP synthesized from Tulasi extract are like crystal flakes, nanohydroxyapatite prepared from eggshells are agglomerated particles and the composite nHA-AgNP contain both crystal flakes and agglomerated particle. The antimicrobial activity of the nanoparticles were evaluated against staphylococcus aureus and Escherichia coli. The biosynthesized nano-composite nHA-AgNP is a cost effective green synthesis route and is useful for removing organics in waste water and enhance environmental protection.

REFERENCES

- 1) Cademartiri, Ludovico; Ozin, Geoffrey (2009). *Concepts of Nanochemistry*. Germany: Wiley VCH. pp. 4–7. [ISBN 978-3527325979](#).
- 2) "Uses of nanoparticles of titanium(IV) oxide (titanium dioxide, TiO₂)". Doc Brown's Chemistry Revision Notes – Nanochemistry.
- 3) Wang, Erkang; Wei, Hui (2013-06-21). "Nanomaterials with enzyme-like characteristics (nanozymes): next-generation artificial enzymes". *Chemical Society Reviews*. **42** (14): 6060–6093. [doi:10.1039/C3CS35486E](#). [ISSN 1460-4744](#). [PMID 23740388](#).
- 4) Kingshott, Peter. "[Electrospun nanofibers as dressings for chronic wound care](#)" (PDF). *Materials Views*. Macromolecular Bioscience.
- 5) Vert, Michel; Doi, Yoshiharu; Hellwich, Karl-Heinz; Hess, Michael; Hodge, Philip; Kubisa, Przemyslaw; Rinaudo, Marguerite; Schué, François (2012). "Terminology for biorelated polymers and applications (IUPAC Recommendations 2012)" (PDF). *Pure and Applied Chemistry*. **84** (2): 377–410. [doi:10.1351/PAC-REC-10-12-04](#). S2CID 98107080
- 6) C.Ciobanu,F.Massuyeau,L.V.constantin and D.Predoi, “Structural and physical Properties of Antibacterial Ag-Doped Nano-hydroxyapatite synthesized at 1000 C”,nanoscale research Letters,vol.6, pp.613-618,December 2011.
- 7) J.H.G Rocha, A.F..Lemos , S. AgathapouloseandJ.M.F.Ferreria, “Hydroxyapatite Scaffolds Hydrothermally Grown From Aragonitic Cuttlefish Bones”,*J.Mater.Chem*,vol.15,pp.5007-5011,October 2005

- 8) R.P.Singh,M.S.Mehta, P. Singh and R. Verma, “In Vitro Performance of Silver-Doped hydroxyapatite Nano Powders -A microstudy”, J Aust Ceram Soc, vol.53,pp.1007-1016
- 9) W. Chen, T. Liu, H.S Courtney, M. Bettenga , C.M Agarwal and J.D. Bumgardner,” In Vitro anti-bacterial And Biological Properties Of Magnetron Co-Sputtered Silver-containing Hydroxyapatite Coating”, J. Biomaterials,vol.27,pp.5512-5517,November 2000
- 10) Bharti, Amardeep, Singh, Suman and Meena ”,Synthesis Of Novel Multiple Shaped Silver Nanoparticles Incorporated Hydroxyapatite Nanocomposite for Orthopaedic Body Implants “,Advanced Science Letters,vol.20 ,pp.1297-1302 July 2014.
- 11) Hussain I, Singh NB, Singh A, et al. Green synthesis of nanoparticles
- 12) S. S. Shankar, A. Ahmad, and M. Sastry, “Geranium leaf assisted biosynthesis of silver nanoparticles,” *Biotechnology Progress*, vol. 19, no. 6, pp. 1627–1631, 2003.View at: [Publisher Site](#) | [Google Scholar](#)
- 13) J. L. Gardea-Torresdey, E. Gomez, J. R. Peralta-Videa, J. G. Parsons, H. Troiani, and M. Jose-Yacaman, “Alfalfa sprouts: a natural source for the synthesis of silver nanoparticles,” *Langmuir*, vol. 19, no. 4, pp. 1357–1361, 2003.View at: [Publisher Site](#) | [Google Scholar](#)

- 14) S. S. Shankar, A. Rai, A. Ahmad, and M. Sastry, "Controlling the optical properties of lemongrass extract synthesized gold nanotriangles and potential application in infrared-absorbing optical coatings," *Chemistry of Materials*, vol. 17, no. 3, pp. 566–572, 2005. View at: [Publisher Site](#) | [Google Scholar](#)
- 15) S. P. Chandran, M. Chaudhary, R. Pasricha, A. Ahmad, and M. Sastry, "Synthesis of gold nanotriangles and silver nanoparticles using Aloe vera plant extract," *Biotechnology Progress*, vol. 22, no. 2, pp. 577–583, 2006. View at: [Publisher Site](#) | [Google Scholar](#)
- 16) J. Huang, Q. Li, D. Sun et al., "Biosynthesis of silver and gold nanoparticles by novel sundried *Cinnamomum camphora* leaf," *Nanotechnology*, vol. 18, no. 10, Article ID 105104, 2007. View at: [Publisher Site](#) | [Google Scholar](#)
- 17) B. Ankamwar, C. Damle, A. Ahmad, and M. Sastry, "Biosynthesis of gold and silver nanoparticles using *Emblica officinalis* fruit extract, their phase transfer and transmetallation in an organic solution," *Journal of Nanoscience and Nanotechnology*, vol. 5, no. 10, pp. 1665–1671, 2005. View at: [Publisher Site](#) | [Google Scholar](#)
- 18) K. B. Narayanan and N. Sakthivel, "Coriander leaf mediated biosynthesis of gold nanoparticles," *Materials Letters*, vol. 62, no. 30, pp. 4588–4590, 2008. View at: [Publisher Site](#) | [Google Scholar](#)
- 19) S. Ankanna, T. N. V. K. V. Prasad, E. K. Elumalai, and N. Savithamma, "Production of biogenic silver nanoparticles using *Boswellia ovalifoliolata* stem bark," *Digest Journal of Nanomaterials and Biostructures*, vol. 5, no. 2, pp. 369–372, 2010. View at: [Google Scholar](#)

- 20) P. Rajasekharreddy, P. U. Rani, and B. Sreedhar, "Qualitative assessment of silver and gold nanoparticle synthesis in various plants: a photobiological approach," *Journal of Nanoparticle Research*, vol. 12, no. 5, pp. 1711–1721, 2010. View at: [Publisher Site](#) | [Google Scholar](#)
- 21) V. Parashar, R. Parashar, B. Sharma, and A. C. Pandey, "Parthenium leaf extract mediated synthesis of silver nanoparticles: a novel approach towards weed utilization," *Digest Journal of Nanomaterials and Biostructures*, vol. 4, no. 1, pp. 45–50, 2009. View at: [Google Scholar](#)
- 22) [Materials Science and Engineering: CVolume 91](#), 1 October 2018, Pages 881-
- 23) S. H. Lim and S. M. Hudson, *Color. Technol.*, **56**, 227 (2004).
- 24) * QL Feng, J Wu, GQ Chen, FZ Cui, TN Kim, JO. Kim *Journal of biomedical materials research*. 52(4), 662 (2000).
- * J. R. EJL Morones, A. Camacho, K., Holt J. B. Kouri, J. T. Ramirez, M. J. Yacaman *Nanotechnology*. 16(10), 2346 (2005).
- * M. YA Rai, A. Gade, *Biotechnology advances.*;27(1):76 (2009).
- *I. S-SB. Sondi, *Journal of colloid and interface science.*;275(1):177 (2004).
- 25) AbdelRahim, K., Mahmoud, S. Y., Ali, A. M., Almaary, K. S., Mustafa, A. E. Z. M. A., &Husseiny, S. M. (2017). *Extracellular biosynthesis of silver nanoparticles using Rhizopusstolonifer. Saudi Journal of Biological Sciences*, 24(1), 208-216. <http://dx.doi.org/10.1016/j.sjbs.2016.02.025> PMid:28053592.
- 26) E. M. Hetrick and M. H. Schoenfisch, "Reducing implantrelated infections: active release strategies," *Chemical Society Reviews*, vol. 35, no. 9, pp. 780–789, 2006.

- 27) S. L. Percival, P. G. Bowler, and D. Russell, "Bacterial resistance to silver in wound care," *Journal of Hospital Infection*, vol. 60, no. 1, pp. 1–7, 2005.
- 28) D. Lee, R. E. Cohen, and M. F. Rubner, "Antibacterial properties of Ag nanoparticle loaded multilayers and formation of magnetically directed antibacterial microparticles," *Langmuir*, vol. 21, no. 21, pp. 9651–9659, 2005.
- 29) I. Sondi and B. Salopek-Sondi, "Silver nanoparticles as antimicrobial agent: a case study on *E. coli* as a model for Gramnegative bacteria," *Journal of Colloid and Interface Science*, vol. 275, no. 1, pp. 177–182, 2004.
- 30) A. R. Shahverdi, A. F. Pharm, H. R. Shahverdi, and S. Minaian, "Synthesis and effect of silver nanoparticles on the antibacterial activity of different antibiotics against *Staphylococcus aureus* and *Escherichia coli*," *Nanomedicine: Nanotechnology, Biology and Medicine*, vol. 3, no. 2, pp. 168–171, 2007.
- 31) A. Panaćek, L. Kvě̇itek, R. Pucek, et al., "Silver colloid nanoparticles: synthesis, characterization, and their antibacterial activity," *Journal of Physical Chemistry B*, vol. 110, no. 33, pp. 16248–16253, 2006.
- 32) K. Dunn and V. Edwards-Jones, Eds., "The role of Acticoat™ with nanocrystalline silver in the management of burns," *Burns*, vol. 30, supplement 1, pp. S1–S9, 2004.
- 33) K.-H. Cho, J.-E. Park, T. Osaka, and S.-G. Park, "The study of antimicrobial activity and preservative effects of nanosilver ingredient," *ElectrochimicaActa*, vol. 51, no. 5, pp. 956–960, 2005

- 34) R. Kumar and H. Munstedt, "Silver ion release from antimicrobial polyamide/silver composites," *Biomaterials*, vol. 26, no. 14, pp. 2081–2088, 2005.
- 35) M. Bellantone, H. D. Williams, and L. L. Hench, "Broad-spectrum bactericidal activity of Ag₂O-doped bioactive glass," *Antimicrobial Agents and Chemotherapy*, vol. 46, no. 6, pp. 1940–1945, 2002.
- 36) V. Alt, T. Bechert, P. Steinrucke, et al., "An in vitro assessment of the antibacterial properties and cytotoxicity of nanoparticulate silver bone cement," *Biomaterials*, vol. 25, no. 18, pp. 4383–4391, 2004.
- 37) V. Sambhy, M. M. MacBride, B. R. Peterson, and A. Sen, "Silver bromide nanoparticle/polymer composites: dual action tunable antimicrobial materials," *Journal of the American Chemical Society*, vol. 128, no. 30, pp. 9798–9808, 2006.
- 38) W. Chen, S. Oh, A. P. Ong, et al., "Antibacterial and osteogenic properties of silver-containing hydroxyapatite coatings produced using a sol gel process," *Journal of Biomedical Materials Research Part A*, vol. 82, no. 4, pp. 899–906, 2007.
- 39) R.-J. Chung, M.-F. Hsieh, K.-C. Huang, L.-H. Perng, F.-I. Chou, and T.-S. Chin, "Anti-microbial hydroxyapatite particles synthesized by a sol-gel route," *Journal of Sol-Gel Science and Technology*, vol. 33, no. 2, pp. 229–239, 2005.
- 40) N. Rameshbabu, T. S. Sampath Kumar, T. G. Prabhakar, V. S. Sastry, K. V. G. K. Murty, and K. Prasad Rao, "Antibacterial nanosized silver substituted hydroxyapatite: synthesis and characterization," *Journal of Biomedical Materials Research Part A*, vol. 80, no. 3, pp. 581–591, 2007.

- 41) I.-H. Han, I.-S. Lee, J.-H. Song, et al., "Characterization of a silver-incorporated calcium phosphate film by RBS and its antimicrobial effects," *Biomedical Materials*, vol. 2, no. 3, pp. S91–S94, 2007
- 42) W. Chen, Y. Liu, H. S. Courtney, et al., "In vitro anti-bacterial and biological properties of magnetron co-sputtered silvercontaining hydroxyapatite coating," *Biomaterials*, vol. 27, no. 32, pp. 5512–5517, 2006.
- 43) S. K. Arumugam, T. P. Sastry, B. Sreedhar, and A. B. Mandal, "One step synthesis of silver nanorods by autoreduction of aqueous silver ions with hydroxyapatite: an inorganicinorganic hybrid nanocomposite," *Journal of Biomedical Materials Research Part A*, vol. 80, no. 2, pp. 391–398, 2007
- 44) Suryanarayana, Challapalli, and M. Grant Norton. *X-ray diffraction: a practical approach*. Springer Science & Business Media, 2013.
- 45) I.Vamsi Krishna Undavalli, ... BhupendraKhandelwal, in *Aviation Fuels*, 2021
- 46) Stokes, Debbie J. (2008). *Principles and Practice of Variable Pressure Environmental Scanning Electron Microscopy (VP-ESEM)*. Chichester: John Wiley & Sons. ISBN 978-0470758748.
- 47) Suzuki, E. (2002). "High-resolution scanning electron microscopy of immunogold-labelled cells by the use of thin plasma coating of osmium". *Journal of Microscopy*. 208 (3): 153–157. doi:10.1046/j.1365-2818.2002.01082.x. PMID 12460446.^ Jump up to:a b c

48) Goldstein, G. I.; Newbury, D. E.; Echlin, P.; Joy, D. C.; Fiori, C.; Lifshin, E. (1981). Scanning electron microscopy and x-ray microanalysis. New York: Plenum Press. ISBN 978-0-306-40768-0